

## Vortex Formation in a Stirred Bose-Einstein Condensate

K. W. Madison, F. Chevy, W. Wohlleben,\* and J. Dalibard

*Laboratoire Kastler Brossel,<sup>†</sup> Département de Physique de l'École Normale Supérieure, 24 rue Lhomond, 75005 Paris, France*  
(Received 1 December 1999)

Using a focused laser beam we stir a Bose-Einstein condensate of  $^{87}\text{Rb}$  confined in a magnetic trap and observe the formation of a vortex for a stirring frequency exceeding a critical value. At larger rotation frequencies we produce states of the condensate for which up to four vortices are simultaneously present. We have also measured the lifetime of the single vortex state after turning off the stirring laser beam.

PACS numbers: 03.75.Fi, 32.80.Lg, 67.40.Db

Rotations in quantum physics constitute a source of counterintuitive predictions and results as illustrated by the famous “rotating bucket” experiment with liquid helium. When an ordinary fluid is placed in a rotating container, the steady state corresponds to a rotation of the fluid as a whole together with the vessel. Superfluidity, first observed in liquid He II, changes dramatically this behavior [1,2]. For a small enough rotation frequency, no motion of the superfluid is observed; while above a critical frequency, lines of singularity appear in its velocity field. These singularities, referred to as vortex filaments, correspond to a quantized circulation of the velocity ( $nh/m$ , where  $n$  is an integer, and  $m$  the mass of a particle of the fluid) along a closed contour around the vortex. In this Letter, we report the observation of such vortices in a stirred gaseous condensate of atomic rubidium. We determine the critical frequency for their formation, and we analyze their metastability when the rotation of the confining “container” is stopped.

The interest in vortices for gaseous condensates is that, due to the very low density, the theory is tractable in these systems and the diameter of the vortex core, which is on the order of the healing length, is typically 3 orders of magnitude larger than in He II. At this scale, further improved by a ballistic expansion, the vortex filament is large enough to be observed optically. The generation of quantized vortices in gaseous samples has been the subject of numerous theoretical studies since the first observations of Bose-Einstein condensation in atomic gases [3–6]. Two schemes have been considered. The first one uses laser beams to engineer the phase of the condensate wave function and produce the desired velocity field [7–11]. Recently this scheme [10] has been successfully applied to a binary mixture of condensates, resulting in a quantized rotation of one of the two components around the second one [12]. Phase imprinting has also been used for the generation of solitons inside a condensate [13,14].

The second scheme, which is explored in the present work, is directly analogous to the rotating bucket experiment [15,16]. The atoms are confined in a static, cylindrically symmetric Ioffe-Pritchard magnetic trap upon which we superimpose a nonaxisymmetric, attractive dipole potential created by a stirring laser beam. The combined potential leads to a cigar-shaped harmonic trap with a slightly

anisotropic transverse profile. The transverse anisotropy is rotated at angular frequency  $\Omega$  as the gas is evaporatively cooled to Bose-Einstein condensation, and it plays the role of the bucket wall roughness.

In this scheme, the formation of vortices is, in principle, a consequence of thermal equilibrium. In the frame rotating at the same frequency as the anisotropy, the Hamiltonian is time independent, and one can use a standard thermodynamics approach to determine the steady state of the system. In this frame, the Hamiltonian can be written  $\tilde{H} = H - \Omega L_z$ , where  $H$  is the Hamiltonian in the absence of rotation, and  $L_z$  is the total orbital angular momentum along the rotation axis. Above a critical rotation frequency,  $\Omega_c$ , the term  $-\Omega L_z$  can favor the creation of a state where the condensate wave function has an angular momentum  $\hbar$  along the  $z$  axis and therefore contains a vortex filament [17–25]. The density of the condensate at the center of the vortex is zero, and the radius of the vortex core is of the order of the healing length  $\xi = (8\pi a\rho)^{-1/2}$ , where  $a$  is the scattering length characterizing the 2-body interaction, and  $\rho$  the density of the condensate [26].

The study of a vortex generated by this second route allows for the investigation of several debated questions such as the fate of the system when the rotating velocity increases above  $\Omega_c$ . This could in principle lead to the formation of a single vortex with  $n > 1$  at the center of the trap; however, this state has been shown to be either dynamically or thermodynamically unstable [1,21–24,27]. The predicted alternative for large rotation frequencies consists of a lattice of  $n = 1$  vortices. Another important issue is the stability of the current associated with the vortex once the rotating anisotropy is removed [28].

Our experimental setup has been described in detail previously [29]. We start with  $10^9$   $^{87}\text{Rb}$  atoms in a magneto-optical trap which are precooled and then transferred into an Ioffe-Pritchard magnetic trap. The evaporation radio frequency starts at  $\nu_{\text{rf}} = 15$  MHz and decreases exponentially to  $\nu_{\text{rf}}^{(\text{final})}$  in 25 s with a time constant of 5.9 s. Condensation occurs at  $\Delta\nu_{\text{rf}} = \nu_{\text{rf}}^{(\text{final})} - \nu_{\text{rf}}^{(\text{min})} \approx 50$  kHz, with  $2.5 \times 10^6$  atoms and a temperature 500 nK. Here  $\nu_{\text{rf}}^{(\text{min})} = 430 (\pm 1)$  kHz is the radio frequency which empties completely the trap. The slow oscillation frequency of the elongated magnetic trap is  $\omega_z/(2\pi) = 11.7$  Hz ( $z$  is

horizontal in our setup), while the transverse oscillation frequency is  $\omega_{\perp}/(2\pi) = 219$  Hz. For a quasipure condensate with  $10^5$  atoms, using the Thomas-Fermi approximation, we find for the radial and longitudinal sizes of the condensate  $\Delta_{\perp} = 2.6 \mu\text{m}$  and  $\Delta_z = 49 \mu\text{m}$ , respectively.

When the evaporation radio frequency  $\nu_{\text{rf}}$  reaches the value  $\nu_{\text{rf}}^{(\text{min})} + 80$  kHz, we switch on the stirring laser beam which propagates along the slow axis of the magnetic trap. The beam waist is  $w_s = 20.0 (\pm 1) \mu\text{m}$  and the laser power  $P$  is 0.4 mW. The recoil heating induced by this far-detuned beam (wavelength 852 nm) is negligible. Two crossed acousto-optic modulators, combined with a proper imaging system, then allow for an arbitrary translation of the laser beam axis with respect to the symmetry axis of the condensate.

The motion of the stirring beam consists of the superposition of a fast and a slow component. The optical spoon's axis is toggled at a high frequency (100 kHz) between two symmetric positions about the trap axis  $z$ . The intersections of the stirring beam axis and the  $z = 0$  plane are  $\pm a(\cos\theta \mathbf{u}_x + \sin\theta \mathbf{u}_y)$ , where the distance  $a$  is  $8 \mu\text{m}$ . The fast toggle frequency is chosen to be much larger than the magnetic trap frequencies so that the atoms experience an effective two-beam, time averaged potential. The slow component of the motion is a uniform rotation of the angle  $\theta = \Omega t$ . The value of the angular frequency  $\Omega$  is maintained fixed during the evaporation at a value chosen between 0 and  $250 \text{ rad s}^{-1}$ .

Since  $w_s \gg \Delta_{\perp}$ , the dipole potential, proportional to the power of the stirring beam, is well approximated by  $m\omega_{\perp}^2(\epsilon_X X^2 + \epsilon_Y Y^2)/2$ . The  $X, Y$  basis is rotated with respect to the fixed axes  $(x, y)$  by the angle  $\theta(t)$ , and  $\epsilon_X = 0.03$  and  $\epsilon_Y = 0.09$  for the parameters given above [30]. The action of this beam is essentially a slight modification of the transverse frequencies of the magnetic trap, while the longitudinal frequency is nearly unchanged. The overall stability of the stirring beam on the condensate appears to be a crucial element for the success of the experiment, and we estimate that our stirring beam axis is fixed to and stable on the condensate axis to within  $2 \mu\text{m}$ . We checked that for  $\Omega < \Omega_c$  the stirring beam does not affect the evaporation.

For the data presented here, the final frequency of the evaporation ramp was chosen just above  $\nu_{\text{rf}}^{(\text{min})}$  ( $\Delta\nu_{\text{rf}} \in [3, 6]$  kHz). After the end of the evaporation ramp, we let the system reach thermal equilibrium in this "rotating bucket" for a duration  $t_r = 500$  ms in the presence of an rf shield  $30$  kHz above  $\nu_{\text{rf}}^{(\text{final})}$ . The vortices induced in the condensate by the optical spoon are then studied using a time-of-flight analysis. We ramp down the stirring beam slowly (in 8 ms) to avoid inducing additional excitations in the condensate, and we then switch off the magnetic field and allow the droplet to fall for  $\tau = 27$  ms. Because of the atomic mean field energy, the initial cigar shape of the atomic cloud transforms into a pancake shape during

the free fall. The transverse  $xy$  and  $z$  sizes grow by a factor of 40 and 1.2, respectively [31]. In addition, the core size of the vortex should expand at least as fast as the transverse size of the condensate [31–33]. Therefore, a vortex with an initial diameter  $2\xi = 0.4 \mu\text{m}$  for our experimental parameters is expected to grow to a size of  $16 \mu\text{m}$ .

At the end of the time-of-flight period, we illuminate the atomic sample with a resonant probe laser for  $20 \mu\text{s}$ . The shadow of the atomic cloud in the probe beam is imaged onto a CCD camera with an optical resolution  $\sim 7 \mu\text{m}$ . The probe laser propagates along the  $z$  axis so that the image reveals the column density of the cloud after expansion along the stirring axis. The analysis of the images, which proceeds along the same lines as in [29], gives access to the number of condensed  $N_0$  and uncondensed  $N'$  atoms and to the temperature  $T$ . Actually, for the present data, the uncondensed part of the atomic cloud is nearly undetectable, and we can give only an upper bound for the temperature  $T < 80$  nK.

Figure 1 shows a series of five pictures taken at various rotation frequencies  $\Omega$ . They clearly show that for fast enough rotation frequencies we can generate one or several (up to 4) "holes" in the transverse density distribution corresponding to vortices. We show for the 0- and 1-vortex cases a cross section of the column density of the cloud along a transverse axis. The 1-vortex state exhibits

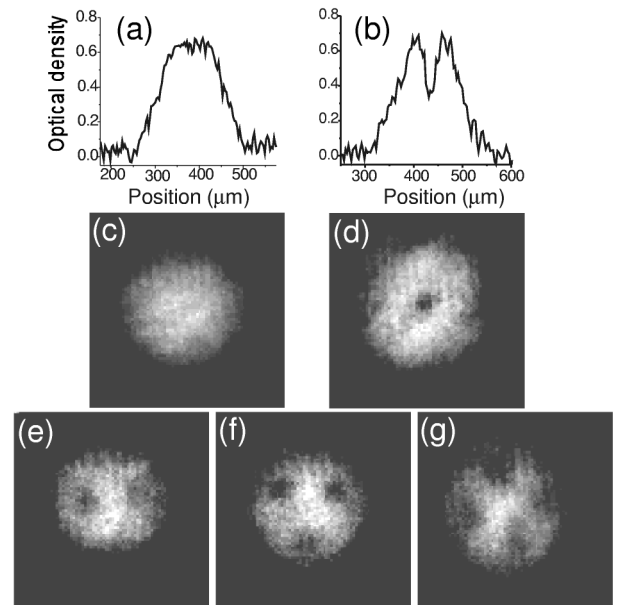


FIG. 1. Transverse absorption images of a Bose-Einstein condensate stirred with a laser beam (after a 27 ms time of flight). For all five images, the condensate number is  $N_0 = (1.4 \pm 0.5) 10^5$  and the temperature is below 80 nK. The rotation frequency  $\Omega/(2\pi)$  is, respectively, (c) 145 Hz, (d) 152 Hz, (e) 169 Hz, (f) 163 Hz, (g) 168 Hz. In (a) and (b) we plot the variation of the optical thickness of the cloud along the horizontal transverse axis for the images (c) (0 vortex) and (d) (1 vortex).

a spectacular dip at the center (up to 50% of the maximal column density) which constitutes an unambiguous signature of the presence of a vortex filament. The diameter of the vortex core following the expansion is measured at the half maximum of the dip to be  $\sim 20 \mu\text{m}$ .

For a systematic study of the vortex stability domain, we have varied in steps of 1 Hz the rotation frequency for a given atom number and temperature. For each frequency, we infer from the absorption image the number of vortices present, and the results are shown in Fig. 2. Below a certain frequency, we always obtain a condensate with no vortices. Then, in a zone with a 2 Hz width, we obtain condensates showing randomly 0 or 1 vortex. Increasing  $\Omega$ , we arrive at a relatively large frequency interval (width 10 Hz) where we systematically observe a condensate with a single vortex present. Our value for the critical frequency is notably larger than the predicted value of 91 Hz [20] (see also [17,19,22,24]). This deviation may be due to the marginality of the Thomas-Fermi approximation for our relatively low condensate number. If  $\Omega$  is increased past the upper edge of the 1-vortex zone, multiple vortices, as shown in Fig. 1, are observed. The range of stability of the multiple vortex zones appears to be much smaller than that for the 1-vortex zone. The 3-vortex zone, for instance, seems to be stable over only 3–4 Hz and is complicated by the occasional appearance of a 2-vortex or a 4-vortex condensate. At this stage of the experiment, it is difficult to determine whether these shot-to-shot fluctuations are due to a lack of experimental reproducibility or to the fact that these various states all have comparable energies and therefore all have a reasonable probability to occur for the range of parameters in question. Finally, when  $\Omega$  is increased past the range of stability for the multiple vortex configuration, the density profile of the condensate takes on a turbulent structure, and the condensate completely disappears for  $\Omega$  larger than 210 Hz, which should be compared with the average transverse frequency of the magnetic + laser dipole potential (226 Hz).

It is remarkable that the multiple vortex configurations most often occur in a symmetric arrangement of the vortex cores: an equilateral triangle and a square for the 3-vortex and the 4-vortex cases, respectively. This finding supports the theoretical analysis of [24], which shows that vortices rotating in the same direction experience an effective repulsive interaction, which in turn favors these stable configurations (see also [21]).

The final question addressed in this Letter concerns the lifetime of a vortex state in an axisymmetric trap. Without

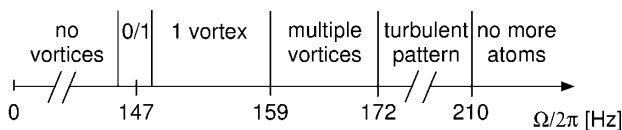


FIG. 2. Edges of the regions of stability for the 0, 1, and multiple vortex configurations. The condensate number is  $N_0 = (2.3 \pm 0.6) 10^5$  and the temperature below 80 nK.

a rotating anisotropy, the vortex state is no longer the lowest energy state of the system, and, after the anisotropy is removed, one expects that the gas will eventually relax to a condensate with no vortex plus a slightly larger thermal component, bolstered by the energy contained in the vortex state. Figure 3 presents the experimental study of the single-vortex state lifetime at two different condensate parameters. We choose a rotation frequency  $\Omega$  in the middle of the 1-vortex range of stability, and we let the vortex form as before in the presence of the stirring beam. Then we switch off the stirring beam, and we allow the gas to evolve in the pure magnetic trap for an adjustable time. Finally, we perform a time-of-flight analysis to determine whether the vortex is present or not. Each point in the two lifetime curves represents the average of 10 shots, where we have plotted the fraction of pictures showing unambiguously a vortex as a function of time [34]. We deduce from this curve a characteristic lifetime of the vortex state in the range 400 to 1000 ms with a clear nonexponential decay behavior. In addition, we observed that at long times the vortex rarely appears well centered as it does immediately after formation.

To summarize, we have reported the formation of vortices in a gaseous Bose-Einstein condensate when it is stirred by a laser beam which produces a slight rotating anisotropy. A natural extension of this work is to study the superfluid aspects of this system [35] by investigating the dynamics for vortex nucleation and decay. An important question is the role of the thermal component. For instance, nucleation can occur either by transfer of angular momentum from this component to the condensate or directly from an instability of the nonvortex state [22,24,36–38]. Also the decay of the single vortex state may be due to the coupling with a nonrotating thermal component [39] or due to the instability induced by the residual, fixed anisotropy of our magnetic trap (measured

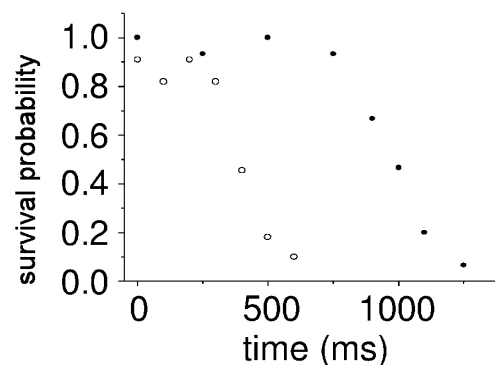


FIG. 3. Fraction of images showing a vortex as a function of the time spent by the gas in the axisymmetric trap after the end of the stirring phase for two condensate conditions. The sets of data correspond to condensate numbers of  $N_0^{(*)} = (2.3 \pm 0.6) 10^5$  and  $N_0^{(\bullet)} = (1.2 \pm 0.3) 10^5$  which were obtained with  $\Delta\nu_{\text{rf}} = 6$  and 3 kHz, respectively. This implies that  $T^{(*)} > T^{(\bullet)}$ , where both temperatures are below our detection limit of 80 nK.

to be  $\omega_x/\omega_y = 1.012 \pm 0.002$ ) [40]. Finally, this type of experiment gives access, in principle, to the elementary excitations of the vortex filament [41–43], the study of which might reveal new aspects of the superfluid properties of these systems.

We thank Y. Castin, C. Cohen-Tannoudji, C. Deroulers, D. Guéry-Odelin, C. Salomon, G. Shlyapnikov, S. Stringari, and the ENS Laser Cooling Group for several helpful discussions and comments. This work was partially supported by CNRS, Collège de France, DRET, DRED, and EC (TMR network ERB FMRX-CT96-0002). This material is based upon work supported by the North Atlantic Treaty Organization under an NSF-NATO grant awarded to K. M. in 1999.

---

\*Permanent address: Max-Planck-Institute für Kernphysik, Heidelberg, Germany.

†Unité de Recherche de l'École normale supérieure et de l'Université Pierre et Marie Curie, associée au CNRS.

- [1] E. M. Lifshitz and L. P. Pitaevskii, *Statistical Physics* (Butterworth-Heinemann, Stoneham, MA, 1980), Part 2, Chap. III.
- [2] R. J. Donnelly, *Quantized Vortices in Helium II* (Cambridge University Press, Cambridge, England, 1991).
- [3] M. H. Anderson *et al.*, *Science* **269**, 198 (1995).
- [4] C. C. Bradley *et al.*, *Phys. Rev. Lett.* **78**, 985 (1997); see also C. C. Bradley *et al.*, *Phys. Rev. Lett.* **75**, 1687 (1995).
- [5] K. B. Davis *et al.*, *Phys. Rev. Lett.* **75**, 3969 (1995).
- [6] D. Fried *et al.*, *Phys. Rev. Lett.* **81**, 3811 (1998).
- [7] K. P. Marzlin *et al.*, *Phys. Rev. Lett.* **79**, 4728 (1997).
- [8] R. Dum *et al.*, *Phys. Rev. Lett.* **80**, 2972 (1998).
- [9] K. G. Petrosyan and L. You, *Phys. Rev. A* **59**, 639 (1999).
- [10] J. Williams and M. Holland, *Nature (London)* **401**, 568 (1999).
- [11] L. Dobrek *et al.*, *Phys. Rev. A* **60**, R3381 (1999).
- [12] M. R. Matthews *et al.*, *Phys. Rev. Lett.* **83**, 2498 (1999).
- [13] S. Burger *et al.*, *cond-mat/9910487*.
- [14] J. Denschlag *et al.*, *Science* **287**, 97 (2000).
- [15] A. J. Leggett, *Topics in Superfluidity and Superconductivity*, in *Low Temperature Physics*, edited by M. Hoch and R. Lemmer (Springer-Verlag, Berlin, 1992).
- [16] S. Stringari, *Phys. Rev. Lett.* **82**, 4371 (1999).
- [17] G. Baym and C. J. Pethick, *Phys. Rev. Lett.* **76**, 6 (1996).
- [18] F. Dalfovo and S. Stringari, *Phys. Rev. A* **53**, 2477 (1996).
- [19] S. Sinha, *Phys. Rev. A* **55**, 4325 (1997).
- [20] E. Lundh *et al.*, *Phys. Rev. A* **55**, 2126 (1997).
- [21] D. Butts and D. Rokhsar, *Nature (London)* **397**, 327 (1999).
- [22] D. Feder *et al.*, *Phys. Rev. Lett.* **82**, 4956 (1999).
- [23] A. Fetter, *J. Low. Temp. Phys.* **113**, 189 (1998).
- [24] Y. Castin and R. Dum, *Eur. Phys. J. D* **7**, 399 (1999).
- [25] B. Caradoc-Davies *et al.*, *Phys. Rev. Lett.* **83**, 895 (1999).
- [26] For a review, see, e.g., F. Dalfovo *et al.*, *Rev. Mod. Phys.* **71**, 463 (1999).
- [27] H. Pu *et al.*, *Phys. Rev. A* **59**, 1533 (1999).
- [28] D. Rokhsar, *Phys. Rev. Lett.* **79**, 2164 (1997).
- [29] J. Söding *et al.*, *Appl. Phys. B* **69**, 257 (1999).
- [30] We observed that the vortex formation is not sensitive to the exact value of  $\epsilon_x, \epsilon_y$ , and a single vortex state under the same conditions was successfully created with a laser power of half and twice the value of 0.4 mW used here.
- [31] Y. Castin and R. Dum, *Phys. Rev. Lett.* **77**, 5315 (1996).
- [32] E. Lundh *et al.*, *Phys. Rev. A* **58**, 4816 (1998).
- [33] F. Dalfovo and M. Modugno, *cond-mat/9907102*.
- [34] To eliminate a possible “psychological bias,” the images were examined in a random order after collection.
- [35] C. Raman *et al.*, *Phys. Rev. Lett.* **83**, 2502 (1999).
- [36] T. Isoshima and K. Machida, *Phys. Rev. A* **60**, 3313 (1999).
- [37] A. Svidzinsky and A. Fetter, *cond-mat/9811348*.
- [38] J. R. Anglin and W. H. Zurek, *Phys. Rev. Lett.* **83**, 1707 (1999).
- [39] P. Fedichev and G. Shlyapnikov, *Phys. Rev. A* **60**, R1779 (1999).
- [40] Our observation that the quantities  $N/T^3$  at the condensation point with and without the rotating spoon (160 Hz) were equal (to within 15%) indicates that the gas was not yet rotating at this stage in the evaporation.
- [41] R. Dodd *et al.*, *Phys. Rev. A* **56**, 587 (1997).
- [42] F. Zambelli and S. Stringari, *Phys. Rev. Lett.* **81**, 1754 (1999).
- [43] A. Svidzinsky and A. Fetter, *Phys. Rev. A* **58**, 3168 (1998).